Journal of Hazardous Materials 195 (2011) 124–131

Contents lists available at ScienceDirect

Journal of Hazardous Materials

journal homepage: www.elsevier.com/locate/jhazmat

Adsorption of volatile organic compounds by metal–organic frameworks MIL-101: Influence of molecular size and shape

Kun Yang[a,b,*], Qian Sun[a,b], Feng Xue[a,b], Daohui Lin[a,b]

[a] Department of Environmental Science, Zhejiang University, Hangzhou 310058, China
[b] Zhejiang Provincial Key Laboratory of Organic Pollution Process and Control, Hangzhou, Zhejiang 310058, China

ARTICLE INFO

Article history:
Received 4 May 2011
Received in revised form 5 August 2011
Accepted 5 August 2011
Available online 11 August 2011

Keywords:
Metal–organic frameworks
MIL-101
VOCs
Adsorption

ABSTRACT

Adsorption of gaseous volatile organic compounds (VOCs) on metal–organic frameworks MIL-101, a novel porous adsorbent with extremely large Langmuir surface area of 5870 m^2/g and pore volume of 1.85 cm^3/g, and the influence of VOC molecular size and shape on adsorption were investigated in this study. We observed that MIL-101 is a potential superior adsorbent for the sorptive removal of VOCs including polar acetone and nonpolar benzene, toluene, ethylbeznene, and xylenes. MIL-101 is of higher adsorption capacities for all selected VOCs than zeolite, activated carbon and other reported adsorbents. Adsorption of VOCs on MIL-101 is captured by a pore filling mechanism, showing the size and shape selectivity of VOC molecules. These prove to be a negative linear relationship between the volume adsorption capacities of VOCs and their molecular cross-sectional area values. Most VOC molecules, such as acetone, benzene, toluene, ethylbenzene and p-xylene, enter into MIL-101 pores with the planes having the minimum diameters. However, m-xylene and o-xylene may fill into the pores with the planes having the maximum diameters because of the preferred interaction of MIL-101 with the two methyl groups of adsorbate molecules.

1. Introduction

Volatile organic compounds (VOCs), including BTEXs (i.e., benzene, toluene, ethylbenzene, and xylenes), aldehydes, ketones, and chlorinated hydrocarbons, are among the most common contaminants in indoor/outdoor air with worldwide concerns [1]. They are largely emitted by the chemical process industries (e.g., thinner, degreasers, cleaners, lubricants, and liquid fuels) and can pose great threat to human being, including sensory irritation symptoms [2], severe disorder of respiratory system or mucous membrane of vision organ [3] and even the cancerization of natural cells [2,4,5]. VOCs in ambient environment may also bring on other serious environmental and health risks such as photochemistry smog [6]. Therefore, a number of add-on-control techniques, including the destruction techniques (e.g., biofiltration, thermal oxidation, and catalytic oxidation) and the recovery techniques (e.g., absorption, adsorption, condensation, and membrane separation), have been developed to control VOCs emissions and to remove VOCs from contaminated air [7]. Among these techniques, adsorption using porous materials as adsorbents is a well-established and effective technique for the removal and recovery of VOCs from air. Porous materials, having large surface area and pore volume, including zeolites [8–10], resins [11], activated carbon together with their derivatives [12–14], are the most frequently utilized adsorbents with high adsorption capacity for VOCs. Efforts are still needed to develop new porous materials with larger surface area and pore volume and higher adsorption capacity for VOC adsorption.

Metal–organic frameworks (MOFs), a new class of hybrid porous solids, are potentially a type of prominent porous adsorbents for VOCs because of the extremely large pore volume and surface area (usually >3000 m^2/g) [15]. MOFs are crystalline hybrid porous solids with ordered three-dimensional network frameworks via strong metal–ligand bonds between metal cations and organic linkers [15,16]. Since their discovery, MOFs received lots of significant attentions in their potential applications in gas storage, separation, heterogeneous catalysis, and sensing [15–17]. In the great family of MOFs, MIL-101 with the formula of $Cr_3F(H_2O)_2OE(O_2C)–C_6H_4–(CO_2)_3{\cdot}nH_2O$ (n is ~25), which is an automated assembly product of chromium nitrate nonahydrates and terephthalic acid, and firstly reported by Ferey and his coworkers in 2005 [18], is a porous material possessing the largest surface area (5900 ± 300 m^2/g) and pore volume (≈2.0 cm^3/g) among the reported porous materials, which make MIL-101 a potential candidate as adsorbent on gas adsorption [18].

Adsorption researches on MIL-101 initially focused on characteristics of H_2 adsorption [19,20]. Later, the adsorption characteristics of other gases, such as CO_2 [21,22], CH_4 [21,22],

* Corresponding author at: Department of Environmental Science, Zhejiang University, Hangzhou 310058, China. Tel.: +86 571 88982589; fax: +86 571 88982590.
E-mail address: kyang@zju.edu.cn (K. Yang).

0304-3894/$ – see front matter © 2011 Elsevier B.V. All rights reserved.
doi:10.1016/j.jhazmat.2011.08.020

H_2S [23], SF_6 [22], C_3H_8 [22], benzene [24,25], toluene [26], n-alkanes [27], and n-butane [28] on MIL-101 were examined. All of these studies indicated that MIL-101 was a potential superior adsorbent for gas adsorption, especially for organic vapors. For example, Chowdhury and co-workers [22] observed that MIL-101 had higher adsorption capacity of C_3H_8 than that of other gases (i.e., CO_2, CH_4, and SF_6). MIL-101 also showed higher adsorption capacity of benzene (i.e., 16.7 mmol/g) than other frequently used adsorbents including SBA-15, HZSM-5 and activated carbon [24]. In addition, MIL-101 was reported to be a very promising candidate for the application of high-resolution capillary gas chromatograph (GC) as the stationary phase in separation of xylene isomers and ethylbenzene due to its superior adsorption characteristics [29].

In addition to the surface characteristics of porous materials, molecular properties, such as the size and shape of VOCs, play a commonly important role in their adsorption on porous materials [8–14,30]. However, as far as we know, very limited studies were conducted to examine the influence of molecular size and shape of VOCs on their adsorption by MIL-101. The relationship between molecular properties of VOCs and their adsorption on MIL-101 has not been established yet [27]. So it became the main objective of this study. Moreover, only the nonpolar VOCs (i.e., C_3H_8, benzene, toluene, n-alkanes, xylene isomers, ethylbenzene and n-butane) were examined for their adsorption by MIL-101 in previous studies [22,24–30]. Polar VOCs (such as acetone, methanol, ethanol, tetrachloroethane, methyl chloride, various chlorohydrocarbons and perfluorocarbons) were also environmentally concerned pollutants in air due to their high toxicity and volatility [7]. However, adsorption characteristics of these polar VOCs by MIL-101 were still not examined. Therefore, in this study, polar acetone and nonpolar BTEXs with various sizes and shapes were selected as adsorbates to examine the adsorption performance of MIL-101 towards polar and nonpolar VOCs as well as the influences of VOC molecular properties. We also hope to establish the relationships between molecule properties of VOCs and their adsorption on MIL-101, and to explore the underlying adsorption mechanisms.

2. Materials and methods

2.1. Chemicals

Chromium nitrate nonahydrates (99+%), terephthalic acid (TPA) (99+%) and fluorhydric acid (HF) (40+%) were purchased from Sinopharm Chemical Reagent Co., Ltd. (China), Acros organic (USA) and Juhua Reagent Co., Ltd. (China), respectively; acetone (98+%), benzene (98+%), toluene (98+%) and ethylbenzene (98+%) were purchased from Hangzhou Chemical Reagent Co., Ltd (China); o-xylene (98+%), p-xylene (98+%) and m-xylene (98+%) were purchased from Sinopharm Chemical Reagent Co., Ltd. (China). These chemicals were used without any further purification. Selected properties of the VOCs [30,31] are listed in Table 1.

2.2. Synthesis of MIL-101

MIL-101, the highly crystallized green powder of the chromium terephthalate, was synthesized according to the method described in the literature [18]. Briefly, 4.0 g Cr $(NO_3)_3$ (0.01 mol), 1.64 g TPA (0.01 mol), 125 μL HF and 70 mL ultrapure water were transformed into a 100 mL Teflon-lined stainless steel autoclave, sealed, heated up to 220 °C for 8 h, and then were slowly cooled down to atmospheric temperature. After that, the green suspension of MIL-101 was filtered by using a stainless steel meshwork (with a diameter of 0.061 mm) to remove the re-crystallized needle-shaped colorless TPA which retained on the meshwork and the MIL-101 suspension passed through the meshwork. The filtrated MIL-101 suspension was sequently centrifuged at $3500 \times g$ (for 15 min to collect the first precipitates of MIL-101) and $8000 \times g$ (for 15 min to collect the second precipitates of MIL-101). And then, the second precipitates of MIL-101 were washed several times with ultrapure water, and dried at 70 °C for 24 h in a hot air oven for the usage of adsorption experiments.

2.3. Characterization of synthesized MIL-101

Adsorption isotherm of nitrogen on MIL-101 was obtained at 77 K by an Autosorb-1MP-VP apparatus (Quantachrome Corp., USA). The MIL-101 was evacuated overnight at 105 °C to remove the water molecules in MIL-101 prior to the nitrogen adsorption experiment. Specific surface area values of MIL-101were calculated by the Brunauer–Emmett–Teller (BET) method and the Langmuir method using adsorption data of nitrogen adsorption isotherm. Pore size of MIL-101 was calculated by the Quenched Solid State Density Functional Theory (QSDFT) method. Powder X-ray diffraction (XRD) pattern of MIL-101 was recorded on a XPert diffractometer (Panalytical Corp., Netherlands) which was operated at 40 kV for Cu Kα ($\lambda = 0.1543$ nm) radiation from 3° to 70° (2θ angle range) with a scan step size of 0.02°. Transmission electron microscope (TEM) images were taken at 80 kV by a JEM-1230 (JEOL Corp., Japan). The thermal stability of MIL-101 was investigated by thermal gravimetric analysis (TGA) with SDT Q600 (AT Corp., USA) by using approximate 7.3 mg sample from 35 °C to 605 °C with a ramping rate of 2.0 °C/min in air atmosphere. Fourier transform infrared (FT-IR) spectrum was determined using Bruker-vector-22 (German) with a range of 500–4000 cm^{-1}. MIL-101 sample for FT-IR analysis was pretreated by grinding power of MIL-101 together with KBr in an agate mortar and then by pressing them into flakes by a tablet machine.

2.4. Adsorption measurements

The vapor-phase adsorptions of BETXs and acetone were carried out at 25 °C on a volumetric adsorption apparatus, i.e., Autosorb-1MP-VP (Quantachrome Corp., USA). This apparatus was modified

Table 1
Selected properties of VOC molecules.

VOCs	ρ[a] (g/mL, 25 °C)	MW[b] (g/mol)	σ[c] (nm^2)	SP[d] (kPa, 25 °C)	X[e]	Y[e]	Z[e]
Acetone	0.786	58	0.270	30.414	6.600	4.129	5.233
Benzene	0.876	78	0.305	12.573	6.628	3.277	7.337
Toluene	0.865	92	0.344	3.776	6.625	4.012	8.252
Ethylbenzene	0.901	106	0.368	1.320	6.625	5.285	9.361
m-Xylene	0.877	106	0.379	1.117	8.994	3.949	7.315
o-Xylene	0.858	106	0.375	0.876	7.269	3.834	7.826
p-Xylene	0.861	106	0.380	0.725	6.618	3.810	9.146

[a] Density.
[b] Molecule weight.
[c] Molecule cross-sectional area, data cited from Ref. [30].
[d] Saturation pressure.
[e] X, Y and Z are the molecular width, thickness and length, respectively, data cited from Ref. [31].

with an additional organic vapor generation system and a heating system. The VOC vapors were generated by the vapor generation system at 50 °C. The constant adsorption temperature was achieved by putting sample cell into water bath in Dewar flask. The MIL-101 in sample cell was evacuated at 105 °C overnight to remove the water molecules in MIL-101 prior to the adsorption experiments. Adsorption equilibrium was assumed to be reached when the vapor pressure drop in sample cell was less than 0.0001 atm (=8 Pa) within 3 min. The vapor pressure in sample cell was measured by using three transducers (i.e., 1 Torr transducer, 10 Torr transducer and 1000 Torr transducer). The accuracy of 1, 10 and 1000 Torr transducers are ±0.15% of reading, ±0.15% of reading and ±0.1% of full scale, respectively. The linearity of 1, 10 and 1000 Torr transducers are ±0.1% of reading, ±0.1% of reading and ±0.05% of full scale, respectively. The resolution of each transducer is 0.000025%. The adsorbed amount of VOCs on MIL-101 for each pressure at adsorption equilibrium was calculated with the ideal gas law (the fundamental principle of the volumetric adsorption method as well as the volumetric adsorption apparatus) by the difference between the pressure at adsorption equilibrium and the initial vapor pressure in sample cell.

3. Results and discussion

3.1. Characteristics of MIL-101

Nitrogen adsorption isotherm of the dehydrated MIL-101 is shown in Fig. 1A. The specific surface area of MIL-101, calculated by the BET method and the Langmuir method, is about 3980 and 5870 m^2/g, respectively. These values are close to the reported val-

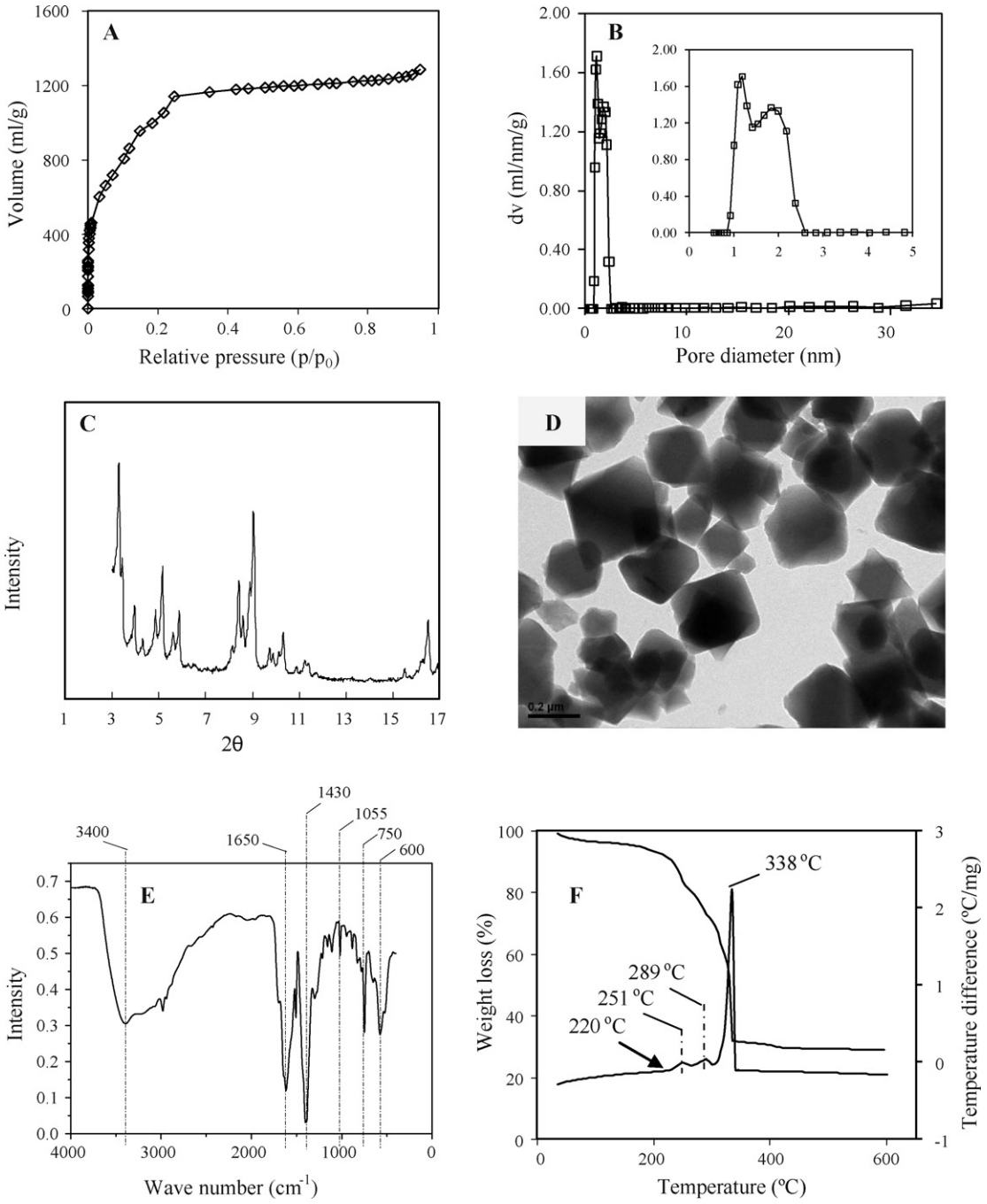

Fig. 1. Nitrogen adsorption isotherm (A), pore size distribution (B), XRD pattern (C), TEM image (D), FT-IR spectrum (E) and DSC/TGA curve (F) of MIL-101.

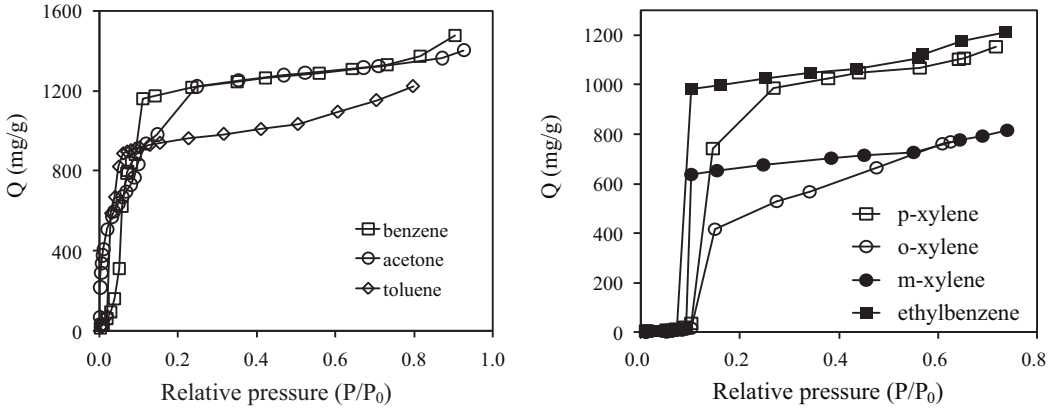

Fig. 2. Isotherms of acetone, benzene, toluene, ethylbenzene and xylenes on MIL-101 at 25 °C.

ues for MIL-101 [18]. The total pore volume of MIL-101 is estimated to be 1.85 cm^3/g at a relative pressure of $P/P_0 = 0.55$. Pore sizes of MIL-101, shown in Fig. 1B, mainly range from 8.5 to 26 Å, and confirm two domain pore sizes (i.e., 12 and 18 Å), which is similar to the pore sizes estimated from the crystal structure [18]. The XRD pattern of the sample obtained (Fig. 1C) is similar to the simulated pattern of MIL-101 reported previously [32]. The TEM image shown in Fig. 1D confirms that the synthesized MIL-101 is a highly crystallized regular octahedron with a perfect cubic symmetry. The FT-IR spectrum of MIL-101 (Fig. 1E) is similar to the previous results [24,29,33]. The strong bands, at 1650 and 1430 cm^{-1}, can be assigned to the vibrational stretching frequencies of the framework (O–C–O), confirming the presence of dicarboxylate linker in the MIL-101 framework [24,33]. The bands at 1055 and 750 cm^{-1} can be assigned to the vibrations of benzene rings [33]. The bands near 600 cm^{-1} are most likely to ascribe to in-plane and out-of-plane bending modes of COO-groups [33]. The TGA profile shows that MIL-101 is stable up to 220 °C (Fig. 1F). A total of 71% weight loss of MIL-101, occurred between 220 and 350 °C, may result from the framework decomposition of the organic moieties [22,24].

3.2. Adsorption characteristics of selected VOCs on MIL-101

Isotherms of acetone, benzene and toluene exhibit a sharp increase of adsorption amount at the relative pressure (P/P_0) less than 0.1 (Fig. 2A). However, there are almost no adsorption of ethylbenzene and xylenes by MIL-101 at $P/P_0 < 0.1$ (Fig. 2B). A sharp increase of adsorption amount of ethylbenzene and xylenes on MIL-101 occurred approximately at P/P_0 from 0.1 to 0.2. The negligible adsorption of ethylbenzene and xylenes on MIL-101 at $P/P_0 < 0.1$ (Fig. 2B) should not be a fact. It may be an artificial result derived from the possibly slow diffusion of ethylbenzene and xylenes into pores of MIL-101 since adsorption equilibrium was assumed to be reached when the pressure drop in sample cell was less than 0.0001 atm (=8 Pa) within 3 min. The low absolute pressure of ethylbenzene and xylenes at $P/P_0 < 0.1$, which is lower than 0.001 atm (=100 Pa) calculated from their P_0 (Table 1), and the big molecular size, which is identified by the large molecule cross-sectional area (Table 1), may be responsible for the slow diffusion of ethylbenzene and xylenes into the pores of MIL-101 [34,35]. Slow diffusion could make the pressure drop of ethylbenzene and xylenes in the sample cell within 3 min undetectable. In addition, the rapid diffusion of acetone, benzene and toluene into the pores of MIL-101, identified by their significant adsorption at $P/P_0 < 0.1$ (Fig. 2A), could be attributed to their smaller molecular sizes as compared with the molecular sizes of ethylbenzene and xylenes [24,34,35]. Another evidence of the slow diffusion and the un-equilibrium of adsorption of ethylbenzene and xylenes is that their desorption isotherms are a litter higher than their adsorption isotherms at $P/P_0 > 0.1$, while the desorption isotherm of acetone with smaller size is almost the same with its adsorption isotherm (Fig. S1 in Supporting Information).

Isotherms of acetone, benzene, toluene, ethylbenzene and xylenes show that adsorption of these VOCs on MIL-101 reached a plateau approximately at $P/P_0 > 0.2$ (Fig. 2). The plateau values (i.e., saturated adsorption capacity) are listed in Table 2. MIL-101 shows the highest adsorption capacity for these VOCs as compared with other commonly utilized adsorbents such as zeolites, resins, activated carbon together with their derivatives [11,24,30,36–44] (Table 2), indicating that MIL-101 is a potential superior adsorbent for the sorptive removal of unwanted VOCs such as polar acetone and apolar BTEXs from contaminated air. For example, the saturated adsorption capacity of benzene on MIL-101 in this study was estimated to be 1291 ± 77 mg/g (i.e., 16.4 mmol/g) at $P/P_0 = 0.55 \pm 0.05$, which is close to the reported value (16.7 mmol/g) of benzene on MIL-101 at $P/P_0 = 0.5$ in a previous study [24] but higher than the saturated adsorption capacity of benzene on HY zeolite (3.3 mmol/g), whose specific surface area is one of the largest among the aluminosilicate zeolites [24], and a pitch-based activated carbon (12.4 mmol/g, the maximum value was reported in the literatures for benzene on adsorbents except for MIL-101) [24].

3.3. Influence of VOC structure on their adsorption into MIL-101 and the underlying adsorption mechanisms

A negative linear relationship between the volume adsorption capacity (V_a) of selected VOCs at $P/P_0 = 0.55 \pm 0.05$ (Table 3) and their molecular cross-sectional area (i.e., the total area of the orthographic projection of a molecule where the molecular geometry is accepted as a sphere) in Table 1 was established (Fig. 3). This phenomenon implies that adsorption of selected VOCs into MIL-101 could be attributed to the continuous micropore filling, an adsorption mechanism suggested by previous studies widely for adsorption of various vapors into porous materials including zeolites, resins, activated carbons and MOFs [9–14,24,25,45]. The dependence of the volume adsorption capacity of VOCs (Table 3) on their molecular cross-sectional area (Table 1 and Fig. 3) but not their minimum dimension (Table 1) could be attributed to the pore type (i.e., cylindrical pore) of MIL-101 [18,31]. The decrease of the volume adsorption capacity of VOCs with the increase of VOC molecular cross-sectional area is a result of that VOC molecules cannot enter into a fraction of MIL-101 cylindrical micropores whose sizes are smaller than the VOC molecular size [31]. Therefore, VOC molecules with larger size presented lower volume adsorption capacity. Another evidence of the micropore filling mechanism for adsorption of VOCs into MIL-101 is that the first derivatives of

Table 2
Adsorption capacities of MIL-101 and other adsorbents for selected VOCs.

Adsorbates	Adsorbents	A_{surf} (m^2/g)	Q_a	V_a (mL/g)	Conditions		Refs.
					C_e	T	
Acetone	PCH	740	4.8 mmol/g	0.354	$0.98P/P_0$	298 K	[30]
	ACFC	1604	595 mg/g	0.752	$0.8P/P_0$	20 °C	[36]
	CDAC	965	381 mg/g	0.481	$0.8P/P_0$	20 °C	[36]
	Y-Zeolite	704	7.2 mmol/g	0.528	0.17 atm	20 °C	[37]
	MIL-101	3980	1291 ± 71 mg/g	1.645 ± 0.090	$0.55 \pm 0.05P/P_0$	25 °C	This work
Benzene	MOF-5	2205	2 mg/g	0.002	440 ppm	25 °C	[38]
	IRMOF-3	1568	56 mg/g	0.064	440 ppm	25 °C	[38]
	MOF-74	632	96 mg/g	0.109	440 ppm	25 °C	[38]
	MOF-177	3875	1 mg/g	0.001	440 ppm	25 °C	[38]
	MOF-199	1264	176 mg/g	0.200	440 ppm	25 °C	[38]
	IRMOF-62	1814	109 mg/g	0.124	440 ppm	25 °C	[38]
	SBA-15	805	3.0 mmol/g	0.269	$0.5P/P_0$	30 °C	[24]
	HZSM-5 zeolite	550	1.9 mmol/g	0.170	$0.5P/P_0$	30 °C	[24]
	Activated carbon	1600	8.0 mmol/g	0.717	$0.5P/P_0$	30 °C	[24]
	NDA-201 resin	855.6	5.2 mmol/g	0.466	10 kPa	303 K	[11]
	ACC-963	1705	7.8 mmol/g	0.668	$0.80P/P_0$	273 K	[39]
	ACFC	1604	634 mg/g	0.719	$0.8P/P_0$	20 °C	[36]
	MIL-101	3900	16.7 mmol/g	1.495	$0.5P/P_0$	30 °C	[24]
	MIL-101	3054	15.5 mmol/g	1.388	55 mbar	288 K	[25]
	MIL-101	3980	1291 ± 77 mg/g	1.477 ± 0.081	$0.55 \pm 0.05P/P_0$	25 °C	This work
Toluene	PCH	740	2.9 mmol/g	0.308	$0.95P/P_0$	298 K	[30]
	ACC-963	1705	6.1 mmol/g	0.645	$0.83P/P_0$	273 K	[39]
	Y-Zeolite	704	1.625 mmol/g	0.172	0.022 atm	20 °C	[37]
	MIL-101	3980	1096 ± 142 mg/g	1.270 ± 0.164	$0.55 \pm 0.05P/P_0$	25 °C	This work
Ethylbenzene	$Zn(BDC)\text{-}(Dabco)_{0.5}$	1450	347 mg/g	0.527	0.1 bar	120 °C	[40,41]
	MOF-5	773	99 mg/g	0.146	2.8 kPa	150 °C	[42]
	MOF-monoclinic	225	5 mg/g	0.007	1.3 kPa	150 °C	[42]
	MIL-47	930	35 wt%	0.526	0.035 bar	130 °C	[42,43]
	PCH	740	4.25 mmol/g	0.434	$0.98P/P_0$	298 K	[30]
	MIL-101	3980	1105 ± 116 mg/g	1.228 ± 0.128	$0.55 \pm 0.05P/P_0$	25 °C	This work
m-Xylene	$Zn(BDC)\text{-}(Dabco)_{0.5}$	1450	345 mg/g	0.511	0.1 bar	120 °C	[40,41]
	MOF-5	773	151 mg/g	0.217	3.0 kPa	150 °C	[42]
	MOF-monoclinic	225	4 mg/g	0.006	1.3 kPa	150 °C	[42]
	MIL-47	930	37 wt%	0.542	0.03 bar	130 °C	[42,43]
	MIL-96	532	0.81 mL/g	0.814	$0.87P/P_0$	30 °C	[44]
	PCH	740	3.5 mmol/g	0.431	$0.97P/P_0$	298 K	[30]
	MIL-101	3980	727 ± 88 mg/g	0.846 ± 0.100	$0.55 \pm 0.05P/P_0$	25 °C	This work
o-Xylene	$Zn(BDC)\text{-}(Dabco)_{0.5}$	1450	338 mg/g	0.505	0.1 bar	120 °C	[40,41]
	MOF-5	773	125 mg/g	0.181	3.4 kPa	150 °C	[42]
	MOF-monoclinic	225	4 mg/g	0.006	1.3 kPa	150 °C	[42]
	MIL-47	930	36 wt%	0.532	0.028 bar	130 °C	[42,43]
	PCH	740	2.6 mmol/g	0.314	$0.85P/P_0$	298 K	[30]
	MIL-101	3980	758 ± 176 mg/g	0.866 ± 0.205	$0.55 \pm 0.05P/P_0$	25 °C	This work
p-Xylene	$Zn(BDC)\text{-}(Dabco)_{0.5}$	1450	342 mg/g	0.506	0.1 bar	120 °C	[40,41]
	MOF-5	773	138 mg/g	0.198	2.5 kPa	150 °C	[42]
	MOF-monoclinic	225	13 mg/g	0.019	1.2 kPa	150 °C	[42]
	MIL-47	930	40 wt%	0.586	0.035 bar	130 °C	[42,43]
	MIL-96	532	0.105 mL/g	0.105	$0.78P/P_0$	30 °C	[44]
	PCH	740	3.4 mmol/g	0.420	$0.98P/P_0$	298 K	[30]
	MIL-101	3980	1067 ± 83 mg/g	1.246 ± 0.096	$0.55 \pm 0.05P/P_0$	25 °C	This work

A_{surf} is the specific surface area calculated using the BET method; Q_a is the reported data of saturation adsorbed amount of VOCs; C_e is the equilibrium concentration (ppm), relative pressure (P/P_0) or absolute pressure (kPa, atm, mbar or bar) at which the reported Q_a values obtained; T is the temperature at which the reported Q_a values obtained; V_a is adsorbed capacity in volume, calculated from Q_a and chemical density ρ (Table 1), by the following equation: $V_a = Q_a/\rho$.

Table 3
Molecule dimension and the possible and determined volume adsorption capacities of selected VOCs into MIL-101.

Compounds	D_{XY} (nm)	$V_{0.55} - V_{XY}$ (mL/g)	D_{YZ} (nm)	$V_{0.55} - V_{YZ}$ (mL/g)	D_{XZ} (nm)	$V_{0.55} - V_{XZ}$ (mL/g)	V_a (mL/g)
Acetone	0.778	1.392	0.666	1.510	0.842	1.228	1.645 ± 0.090
Benzene	0.739	1.393	0.804	1.291	0.989	1.078	1.477 ± 0.081
Toluene	0.775	1.291	0.918	1.138	1.058	0.918	1.270 ± 0.164
Ethylbenzene	0.847	1.288	1.075	0.997	1.147	0.928	1.228 ± 0.128
m-Xylene	0.982	1.084	0.831	1.228	1.159	0.918	0.846 ± 0.100
o-Xylene	0.822	1.260	0.871	1.228	1.068	1.003	0.866 ± 0.205
p-Xylene	0.746	1.357	0.991	1.075	1.129	0.945	1.246 ± 0.096

$V_{0.55}$ is the adsorbed volume of N_2 into MIL-101 at $P/P_0 = 0.55$; D_{XY}, D_{YZ}, D_{XZ} are diameters of circumcircles of the XY, YZ and XZ plane of molecules, calculated by the following equations: $D_{XY} = (X^2 + Y^2)^{0.5}$, $D_{YZ} = (Y^2 + Z^2)^{0.5}$, $D_{XZ} = (X^2 + Z^2)^{0.5}$, where X, Y and Z are the molecular width, thickness and length (Table 1), respectively; V_{XY}, V_{YX} and V_{XZ} are the adsorbed volumes of N_2 into MIL-101 pores whose sizes are smaller than D_{XY}, D_{YZ} and D_{XZ}, respectively; V_{XY}, V_{YX} and V_{XZ} are obtained directly from the relationship between pore diameter and accumulative pore volume of N_2 on MIL-101(please see the detailed illustration in Supporting Information); V_a is the adsorbed capacity in volume (Table 2).

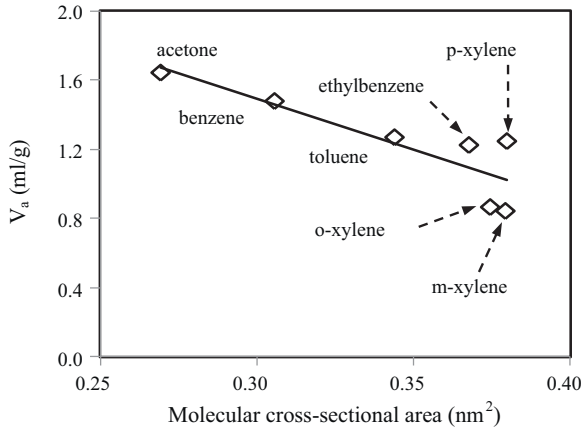

Fig. 3. Relationship between molecular cross-sectional area and volume adsorption capacity (V_a) of seven selected VOCs.

adsorption amount of benzene and toluene, as an example, present two peaks (Fig. 4). The two peaks ascribe to the presence of the two types of microporous windows existed in the skeleton of MIL-101 [46], which can be detected in the bimodal pore size distribution shown in Fig. 1B. The high and low peaks in Fig. 4 could be resulted from the filling of VOC molecules into 12 and 18 Å micropores of MIL-101 (Fig. 1B), respectively.

In addition to molecule size, shape of VOC molecules may also affect their adsorption into MIL-101. For example, m-xylene and o-xylene have almost equal molecule cross-sectional area to p-xylene, but lower adsorption capacity than p-xylene (Fig. 4). This could be attributed to the position difference of methyl side chains in xylene molecules and the consequent difference in molecule shape [47]. For VOC molecules, their shape is commonly accepted as rectangular solid, having three important dimensions, i.e., the width (X), thickness (Y) and length (Z) (Table 1). The rectangular VOC molecule is made of six rectangle planes. The six rectangle planes come in three congruent pairs, i.e., XY, YZ and XZ (Table 1), respectively. Therefore, they could possibly enter into pores of MIL-101 with one of the three congruent rectangle pairs. Adsorption capacity of VOCs by filling into pores of MIL-101 is dependent on the length of diagonal line of the molecular rectangle plane (i.e., the diameter of circumcircle of the plane including D_{XY}, D_{YZ} and D_{XZ} listed in Table 3) by which VOC molecules entered into MIL-101 pores since VOC molecules cannot enter into pores whose diameters smaller than the diameter of VOC molecule plane. Mostly, VOC molecules, such as acetone, benzene, toluene, ethylbenzene and p-xylene, enter into MIL-101 pores with the plane having the minimum diameter (i.e., YZ plane of acetone and XY plane of benzene, toluene, ethylbenzene and p-xylene) [48], showing that $V_{0.55} - V_{YZ}$ value of acetone and $V_{0.55} - V_{XY}$ values of toluene, benzene, ethylbenzene and p-xylene are respectively equal to their V_a values (Table 3). However, V_a values of o-xylene and m-xylene are respectively equal to their $V_{0.55} - V_{XZ}$ values, implying that they fill into MIL-101 pores with the XZ plane (i.e., the plane having maximum diameter) (Table 3). A possible reason is that methyl groups of xylene molecules, prior to their benzene ring, interact with active sites of MIL-101 [47], and thus, o-xylene and m-xylene could not fill into the pores with diameters smaller than their D_{XZ} (i.e., the diameter of the maximum plane of o-xylene and m-xylene which depends on the distance between the two methyl groups) as shown in Fig. 5. However, the two methyl groups in p-xylene, linking benzene ring with an angle of about 180°, form a line-type structure, and which allow p-xylene molecules, as similar to ethylbenzene

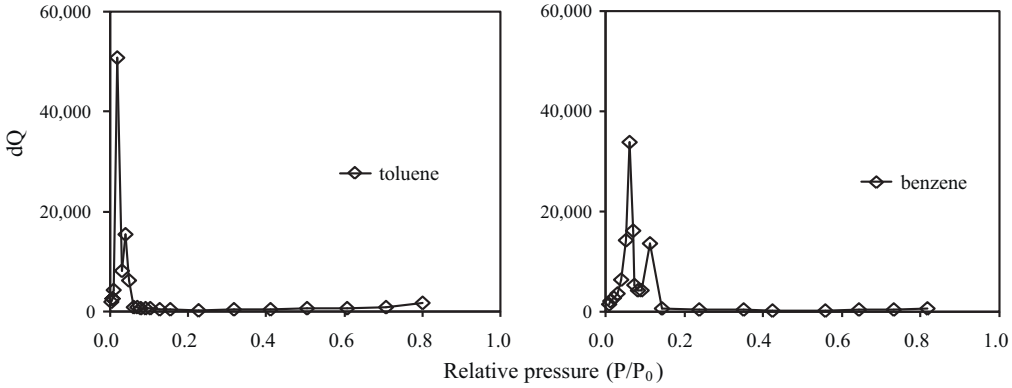

Fig. 4. First derivative (dQ) of adsorption amount of toluene and benzene into MIL-101 versus the relative pressure (P/P_0).

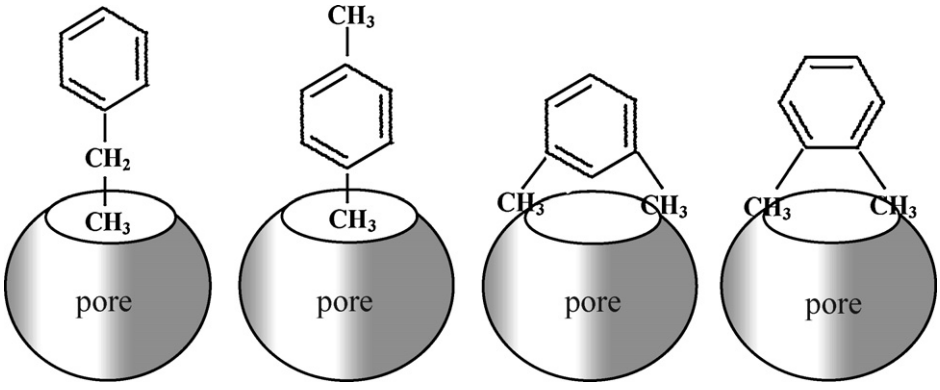

Fig. 5. Scheme of ethylbenzene, p-xylene, o-xylene and m-xylene entering into MIL-101 pores.

molecules, to enter into MIL-101 pores with diameters larger than D_{XY} as shown in Fig. 5. Therefore, volume adsorption capacity of p-xylene in MIL-101 was higher than that of m-xylene and o-xylene (Fig. 3).

4. Conclusions

The results presented that the porous MIL-101 material is a potential superior adsorbent for sorptive removal of unwanted VOCs from contaminated air due to its large surface area and pore volume. Adsorption of VOCs by MIL-101 is captured by a pore filling mechanism, showing the size and shape selectivity of VOC molecules. These prove to be a negative linear relationship between the volume adsorption capacities of selected VOCs and their molecular cross-sectional area values. Mostly, VOC molecules, such as acetone, benzene, toluene, ethylbenzene and p-xylene, entered into MIL-101 pores with the planes having the minimum diameters. However, m-xylene and o-xylene entered into the MIL-101 pores with the molecular planes having the maximum diameters (i.e., D_{XZ}, which depends on the distance between the two methyl groups) because of the preferred interaction of MIL-101 with the two methyl groups of VOC molecules. In addition, the size and shape selectivity of VOC molecules into MIL-101 pores should be mentioned in the application of MIL-101 as an adsorbent for the removal and recovery of VOCs from air.

Acknowledgements

This work was in part supported by the National High Technology Research and Development Program of China (Nos. 2010AA064902 and 2007AA061402), the Science and Technology Department of Zhejiang Province (2006R10022) and the Key Innovation Team for Science and Technology of Zhejiang Province (2009R50047).

Appendix A. Supplementary data

Supplementary data associated with this article can be found, in the online version, at doi:10.1016/j.jhazmat.2011.08.020.

References

[1] WHO, Indoor air quality: organic pollutants, Euro Reports and Studies No. 111, 1989.
[2] P. Wolkoff, C.K. Wilkins, P.A. Clausen, G.D. Nielsen, Organic compounds in office environments—sensory irritation, odor, measurements and the role of reactive chemistry, Indoor Air 16 (2006) 7–19.
[3] J.A. Bernstein, N. Alexis, H. Bacchus, I.L. Bernstein, P. Fritz, E. Horner, N. Li, S. Mason, A. Nel, J. Oullette, K. Reijula, T. Reponen, J. Seltzer, A. Smith, S.M. Tarlo, The health effects of nonindustrial indoor air pollution, J. Allergy Clin. Immunol. 121 (2008) 585–591.
[4] H. Geiger, K.H. Becker, P. Wiesen, Effect of gasoline formulation on the formation of photosmog: a box model study, J. Air Waste Manage. Assoc. 53 (2003) 425–433.
[5] J.E. Cometto-Muniz, W.S. Cain, M.H. Abraham, Detection of single and mixed VOCs by smell and by sensory irritation, Indoor Air 14 (2004) 108–117.
[6] A.E. Pouli, D.G. Hatzinikolaou, C. Piperi, A. Stavridou, M.C. Psallidopoulos, J.C. Stavrides, The cytotoxic effect of volatile organic compounds of the gas phase of cigarette smoke on lung epithelial cells, Free Radic. Biol. Med. 34 (2003) 345–355.
[7] F.I. Khan, A.K. Ghoshal, Removal of volatile organic compounds from polluted air, J. Loss Prevent. Process Ind. 13 (2000) 527–545.
[8] V.R. Choudhary, K. Mantri, Adsorption of aromatic hydrocarbons on highly siliceous MCM-41, Langmuir 16 (2000) 7031–7037.
[9] J. Pires, A. Carvalho, M.B. de Carvalho, Adsorption of volatile organic compounds in Y zeolites and pillared clays, Micropor. Mesopor. Mater. 43 (2001) 277–287.
[10] H.F. Cheng, M. Reinhard, Sorption of trichloroethylene in hydrophobic micropores of dealuminated Y zeolites and natural minerals, Environ. Sci. Technol. 40 (2006) 7694–7701.
[11] P. Liu, C. Long, Q.F. Li, H.M. Qian, A.M. Li, Q.X. Zhang, Adsorption of trichloroethylene and benzene vapors onto hypercrosslinked polymeric resin, J. Hazard. Mater. 166 (2009) 46–51.
[12] D. Das, V. Gaur, N. Verma, Removal of volatile organic compound by activated carbon fiber, Carbon 42 (2004) 2949–2962.
[13] M. Lordgooei, M.J. Rood, M. Rostam-Abadi, Modeling effective diffusivity of volatile organic compounds in activated carbon fiber, Environ. Sci. Technol. 35 (2001) 613–619.
[14] A. Aizpuru, L. Malhautier, J.C. Roux, J.L. Fanlo, Biofiltration of a mixture of volatile organic compounds on granular activated carbon, Biotechnol. Bioeng. 83 (2003) 479–488.
[15] S.T. Meek, J.A. Greathouse, M.D. Allendorf, Metal–organic frameworks: a rapidly growing class of versatile nanoporous materials, Adv. Mater. 23 (2011) 249–267.
[16] J.L.C. Rowsell, O.M. Yaghi, Metal–organic frameworks: a new class of porous materials, Micropor. Mesopor. Mater. 73 (2004) 3–14.
[17] M.B. Sander, L. Pan, X.Y. Huang, J. Li, M. Smith, E. Bittner, B. Bockrath, Microporous metal organic materials: promising candidates as sorbents for hydrogen storage, J. Am. Chem. Soc. 130 (2004) 8–1309.
[18] G. Ferey, C. Mellot-Draznieks, C. Serre, F. Millange, J. Dutour, S. Surble, I. Margiolaki, A chromium terephthalate-based solid with unusually large pore volumes and surface area, Science 309 (2005) 2040–2042.
[19] M. Latroche, S. Surble, C. Serre, C. Mellot-Draznieks, P.L. Llewellyn, J.H. Lee, J.S. Chang, S.H. Jhung, G. Ferey, Hydrogen storage in the giant-pore metal–organic frameworks MIL-100 and MIL-101, Angew. Chem. Int. Edit. 45 (2006) 8227–8231.
[20] Y.W. Li, R.T. Yang, Hydrogen storage in metal–organic and covalent-organic frameworks by spillover, AICHE J. 54 (2008) 269–279.
[21] P.L. Llewellyn, S. Bourrelly, C. Serre, A. Vimont, M. Daturi, L. Hamon, G. De Weireld, J.S. Chang, D.Y. Hong, Y.K. Hwang, S.H. Jhung, G. Ferey, High uptakes of CO_2 and CH_4 in mesoporous metal–organic frameworks MIL-100 and MIL-101, Langmuir 24 (2008) 7245–7250.
[22] P. Chowdhury, C. Bikkina, S. Gumma, Gas adsorption properties of the chromium-based metal organic framework MIL-101, J. Phys. Chem. C 113 (2009) 6616–6621.
[23] L. Hamon, C. Serre, T. Devic, T. Loiseau, F. Millange, G. Ferey, G. De Weireld, Comparative study of hydrogen sulfide adsorption in the MIL-53(Al, Cr, Fe), MIL-47(V), MIL-100(Cr), and MIL-101(Cr) metal–organic frameworks at room temperature, J. Am. Chem. Soc. 131 (2009) 8775–8777.
[24] S.H. Jhung, J.H. Lee, J.W. Yoon, C. Serre, G. Ferey, J.S. Chang, Microwave synthesis of chromium terephthalate MIL-101 and its benzene sorption ability, Adv. Mater. 19 (2007) 121–124.
[25] Z.X. Zhao, X.M. Li, S.S. Huang, Q.B. Xia, Z. Li, Adsorption and diffusion of benzene on chromium-based metal organic framework MIL-101 synthesized by microwave irradiation, Ind. Eng. Chem. Res. 50 (2011) 2254–2261.
[26] C.Y. Huang, M. Song, Z.Y. Gu, H.F. Wang, X.P. Yan, Probing the adsorption characteristic of metal–organic framework MIL-101 for volatile organic compounds by quartz crystal microbalance, Environ. Sci. Technol. 45 (2011) 4490–4496.
[27] T.K. Trung, N.A. Ramsahye, P. Trens, N. Tanchoux, C. Serre, F. Fajula, G. Ferey, Adsorption of C5–C9 hydrocarbons in microporous MOFs MIL-100(Cr) and MIL-101(Cr): a manometric study, Micropor. Mesopor. Mater. 134 (2010) 134–140.
[28] N. Klein, A. Henschel, S. Kaskel, n-Butane adsorption on Cu-3(btc)(2) and MIL-101, Micropor. Mesopor. Mater. 129 (2010) 238–242.
[29] Z.Y. Gu, X.P. Yan, Metal–organic framework MIL-101 for high-resolution gas-chromatographic separation of xylene isomers and ethylbenzene, Angew. Chem. Int. Edit. 49 (2010) 1477–1480.
[30] F. Qu, L.Z. Zhu, K. Yang, Adsorption behaviors of volatile organic compounds (VOCs) on porous clay heterostructures (PCH), J. Hazard. Mater. 170 (2009) 7–12.
[31] C.E. Webster, R.S. Drago, M.C. Zerner, Molecular dimensions for adsorptives, J. Am. Chem. Soc. 120 (1998) 5509–5516.
[32] A. Henschel, K. Gedrich, R. Kraehnert, S. Kaskel, Catalytic properties of MIL-101, Chem. Commun. 419 (2008) 2–4194.
[33] N.V. Maksimchuk, M.N. Timofeeva, M.S. Melgunov, A.N. Shmakov, Y.A. Chesalov, D.N. Dybtsev, V.P. Fedin, O.A. Kholdeeva, Heterogeneous selective oxidation catalysts based on coordination polymer MIL-101 and transition metal-substituted polyoxometalates, J. Catal. 257 (2008) 315–323.
[34] J.G. Bell, X.B. Zhao, Y. Uygur, K.M. Thomas, Adsorption of chloroaromatic models for dioxins on porous carbons: the influence of adsorbate structure and surface functional groups on surface interactions and adsorption kinetics, J. Phys. Chem. C 115 (2011) 2776–2789.
[35] M.B. Sweatman, N. Quirke, W. Zhu, R. Kapteijn, Analysis of gas adsorption in Kureha active carbon based on the slit-pore model and Monte–Carlo simulations, Mol. Simul. 32 (2006) 513–522.
[36] D. Ramirez, S.Y. Qi, M.J. Rood, Equilibrium and heat of adsorption for organic vapors and activated carbons, Environ. Sci. Technol. 39 (2005) 5864–5871.
[37] J.H. Kim, S.J. Lee, M.B. Kim, J.J. Lee, C.H. Lee, Sorption equilibrium and thermal regeneration of acetone and toluene vapors on an activated carbon, Ind. Eng. Chem. Res. 46 (2007) 4584–4594.
[38] D. Britt, D. Tranchemontagne, O.M. Yaghi, Metal–organic frameworks with high capacity and selectivity for harmful gases, Proc. Natl. Acad. Sci. U.S.A. 105 (2008) 11623–11627.
[39] M.E. Ramos, P.R. Bonelli, A.L. Cukierman, M.M.L.R. Carrott, P.J.M. Carrott, Adsorption of volatile organic compounds onto activated carbon cloths derived from a novel regenerated cellulosic precursor, J. Hazard. Mater. 177 (2010) 175–182.
[40] M.P.M. Nicolau, P.S. Barcia, J.M. Gallegos, J.A.C. Silva, A.E. Rodrigues, B.L. Chen, Single- and multicomponent vapor-phase adsorption of xylene isomers and

ethylbenzene in a microporous metal–organic framework, J. Phys. Chem. C 113 (2009) 13173–13179.
[41] D.N. Dybtsev, H. Chun, K. Kim, flexible. Rigid, A highly porous metal–organic framework with unusual guest-dependent dynamic behavior, Angew. Chem. Int. Edit. 43 (2004) 5033–5036.
[42] Z.Y. Gu, D.Q. Jiang, H.F. Wang, X.Y. Cui, X.P. Yan, Adsorption and separation of xylene isomers and ethylbenzene on two Zn-terephthalate metal–organic frameworks, J. Phys. Chem. C 114 (2010) 311–316.
[43] V. Finsy, H. Verelst, L. Alaerts, D. De Vos, P.A. Jacobs, G.V. Baron, J.F.M. Denayer, Pore-filling-dependent selectivity effects in the vapor-phase separation of xylene isomers on the metal–organic framework MIL-47, J. Am. Chem. Soc. 130 (2008) 7110–7118.
[44] J.S. Lee, S.H. Jhung, Vapor-phase adsorption of alkylaromatics on aluminum–trimesate MIL-96: an unusual increase of adsorption capacity with temperature, Micropor. Mesopor. Mater. 129 (2010) 274–277.
[45] I. Senkovska, S. Kaskel, High pressure methane adsorption in the metal–organic frameworks Cu-3(btc)(2), Zn-2(bdc)(2)dabco, and Cr3F(H2O)(2)O(bdc)(3), Micropor. Mesopor. Mater. 112 (2008) 108–115.
[46] D.Y. Hong, Y.K. Hwang, C. Serre, G. Ferey, J.S. Chang, Porous chromium terephthalate MIL-101 with coordinatively unsaturated sites: surface functionalization, encapsulation, sorption and catalysis, Adv. Funct. Mater. 19 (2009) 1537–1552.
[47] G.Q. Guo, H. Chen, Y.C. Long, Separation of p-xylene from C-8 aromatics on binder-free hydrophobic adsorbent of MFI zeolite. I. Studies on static equilibrium, Micropor. Mesopor. Mater. 39 (2000) 149–161.
[48] A.M. Tolmachev, D.A. Firsov, T.A. Kuznetsova, K.M. Anuchin, DFT modeling of the adsorption of benzene, methanol, and ethanol molecules in activated carbon nanopores, Prot. Met. Phys. Chem. Surf. 45 (2009) 163–168.